Comparison of a GH74 xyloglucanase and its CBM-deleted variant from *Thielavia terrestris* and their roles in xyloglucan-rich biomass degradation

Beibei Wang
Nanjing Forestry University
Kaixiang Chen
Nanjing Forestry University
Peiyu Zhang
Nanjing Forestry University
Liangkun Long
Nanjing Forestry University
Shaojun Ding (dshaojun@hotmail.com)
Nanjing Forestry University

Research Article

Keywords: Glycoside hydrolase family 74 (GH74) Xyloglucanase, Family 1 carbohydrate binding module (CBM1), Xyloglucan, Synergism, Lignocellulosic biomass

Posted Date: March 7th, 2022

DOI: https://doi.org/10.21203/rs.3.rs-1417417/v1

Abstract

Background

The hydrolysis of lignocellulose was greatly hindered by the associated hemicellulose. Xyloglucan (XG) is a major complex hemicellulose in the primary plant cell wall, however, the blocking effect of xyloglucan on lignocellulose biodegradation was still less understood compared with xylan and mannan. Glycoside hydrolase family 74 (GH74) enzymes are specific xyloglucanases widely distributed in bacteria and fungi. Fungal GH74 xyloglucanases generally contains family 1 carbohydrate binding module (CBM1), but its effect on the enzymatic properties of GH74 xyloglucanases and its roles in xyloglucan-rich biomass degradation has not been investigated in depth.

Results

*Tt*GH74 and CBM-deleted variant (*T*tGH74ΔCBM) from *Thielavia terrestris* had the same optimum temperature and pH, but *Tt*GH74ΔCBM had higher thermostability. *Tt*GH74 displayed high binding affinity on xyloglucan and cellulose, while *Tt*GH74ΔCBM almost completely lost the adsorption capacity on cellulose. Their hydrolysis action alone or combined with other glycoside hydrolases on the free XG, xyloglucan-coated phosphoric acid swollen cellulose or pretreated corn bran and apple pomace was compared in this study. CBM1 might not be essential for hydrolysis of free XG, but effective for the associated XG to some extent. *Tt*GH74 was more effective in hydrolysis of xyloglucan in corn bran, while *Tt*GH74ΔCBM showed relatively higher catalytic activity on apple pomace. Similar phenomenon was also observed when *Tt*GH74 or *Tt*GH74ΔCBM synergistically acting with CBH1/EG1 mixture. The addition of *Tt*GH74 or *Tt*GH74ΔCBM in CBH1/EG1 mixture significantly facilitated the overall hydrolysis of pretreated corn bran and apple pomace by 1.22–2.02 folds in terms of the degree of synergy. The extra addition of GH10 xylanase in *Tt*GH74 or *Tt*GH74ΔCBM /CBH1/EG1 mixture further improved the overall hydrolysis efficiency, and the degree of synergy was up to 1.50–2.16 because of co-existence of xyloglucan and xylan in pretreated corn bran and apple pomace.

Conclusions

*Tt*GH74 can remove the bound xyloglucan on cellulose, therefore efficiently boost the hydrolysis of the pretreated lignocellulosic biomass by synergistic action with cellulase and xylanase. The presence of CBM1 in *Tt*GH74 is conducive to enzymatic hydrolysis, but its role and significance is substrate-specific due to the differences of xyloglucan contents and structure in various biomasses.

Background

Lignocellulosic biomass has become a potential feedstock for biofuels and biochemicals production, which mainly consists cellulose (25–50%), hemicellulose (15–35%) and lignin (5–30%) with small amounts of pectin and wall proteins (1, 2). Cellulose, the principal component of lignocellulosic biomass, exists as unbranched long fibers composed of β-D-(1, 4)-linked glucan. The cellulose microfibers in lignocellulose are embedded in the matrix composed of hemicellulose, acidic pectin polysaccharide, structural glycoprotein and lignin (3, 4). Hemicelluloses are closely associated with the cellulose fibrils and lignin which greatly hinders the cellulose hydrolysis. Hemicelluloses can be divided into four groups: xylan, mannan, xyloglucan and mixed linkage β-glucan (5). Among them, xyloglucan (XG) is a major complex polysaccharide in the primary cell walls of most of higher plants, and it is

closely associated with cellulose and covers part of the cellulose surface (6, 7). In addition, XG not only has hydrogen bond with cellulose, but also has ester bonds to the —COOH groups of pectin and benzyl-sugar ether bonds to ferulic acid (7). XG have a β-1,4-glucan backbone that is highly branched with α-xylose residues linked to glucose at the O-6 position. The side chain xylosyl residues can be further substituted with different monosaccharide, disaccharide, or trisaccharides. A nomenclature for xyloglucan-derived oligosaccharides was firstly introduced by Fry et al (8). The letter G indicates an unbranched glucose residue, and X denotes the α-D-xylose-(1–6)-β-D-glucose motif in the xylosylated glucan backbone. Xylose residues can carry a β-D-galactose (L motif), or an α-L-arabinose (S motif), while galactose residues in L carry α-L-fucose (F motif), etc. (9)

The bioconversion of lignocellulosic biomass into biofuels and biochemicals needs three steps: (1) pretreatment to improve the accessibility of lignocellulose, (2) enzymatic saccharification to produce fermentable sugars, and (3) microbial fermentation to obtain the target products (10). The hydrolytic efficiency and cost of enzymes in the second step are major factors restricting the cost-effective production of biofuels and biochemicals from lignocellulose due to biomass recalcitrance (11). In view of the complex and strong network structure formed by XG with other lignocellulosic components, XG is very difficult to be removed during common pretreatment, and may be still remained in the pretreated lignocellulosic biomasses, therefore limiting the accessibility and hydrolysis efficiency of cellulase to cellulose (12, 13). The removal of XG is needed to promote the enzymatic hydrolysis of pretreated lignocellulose. Xyloglucanases were widely distributed in bacteria and fungi, and usually co-expressed with cellulase and xylanase (14–16), indicating that they may have synergy with cellulase and xylanase for the efficient hydrolysis of lignocellulose biomass. Previous experiments showed that by adding the so-called accessory enzyme xyloglucanase to the cellulase mixture, the hydrolytic performance of the cellulase mixture on pretreated biomass (including corn stover, corn fiber, sweet sorghum bagasse, barley straw, reed canary grass and willow) can be greatly improved (17, 18). However, compared to the extensive studies of influence of xylan and mannan in overall lignocellulose hydrolysis (19–22), the effect of XG on the overall lignocellulose hydrolysis is still less understood and the role of xyloglucanases need to be elucidated in depth.

Microbial xyloglucanase was first discovered from the *Aspergillus aculeatus* in 1999 (23). Xyloglucanases have been classified into glycoside hydrolase (GH) families 5, 9, 12, 16, 44, 45 and 74 in the Carbohydrate-Active Enzymes (CAZy, http://www.cazy.org/) database (24). Most of the xyloglucanases from fungi belong to GH12 and GH74 (25). Of these, xyloglucanases belonging to GH74 are known to have high specific activity towards XG. GH74 xyloglucanases consist of two seven-bladed β-propeller domains that form a large interfacial cleft to accommodate the bulky polysaccharide (26). GH74 xyloglucanases have been identified and divided into three modes of activity: *exo*, *endo*-dissociative, and *endo*-processive. *Exo*-xyloglucanases recognize the reducing ends of XG and releases two glycosyl residue segments. Both *endo*-xyloglucanases hydrolyze the internal β-1,4-glucan backbone of XG in the initial stage. The difference is that *endo*-processive-xyloglucanases can progressively hydrolyze the XG chain before desorption. In contrast, *endo*-dissociative-xyloglucanases hydrolyze the backbone of XG and release both new chain ends, subsequently, desorption from the XG polysaccharide (26, 27).

The carbohydrate binding modules (CBMs) are non-catalytic modules (28), which have several global roles in functionality, including coordinated glycan recognition, general substrate adherence, and structure–function contributions to the catalytic site (29). According to CAZy database (http://www.cazy.org/), about 60% of GH74 gene structures from fungi contain family 1 carbohydrate binding module (CBM1). CBM1 belongs to surface binding CBM (type A) (30), can interacts with insoluble and crystalline polysaccharides and target the enzymes to the substrate surface, thus, enhance the enzymatic activity (31, 32). At present, there is few literatures in the effect

of CBM1 on GH74 xyloglucanase functionality. It is not clear how CBM1 affects the substrate binding and enzymatic hydrolysis efficiency of GH74 xyloglucanases when degrading XG in lignocellulose.

Thielavia terrestris is a thermophilic filamentous fungus, and can grow normally at 40–50 ℃. It contains a variety of heat-resistant cellulose/hemicellulose hydrolases and has the ability to hydrolyze a variety of major polysaccharides in biomass (33). This strain is a potential source of enzymes with scientific and commercial interests (34). In this study, GH74 xyloglucanase from *T. terrestris* (*Tt*GH74) and its CBM1-deleted variant (*Tt*GH74ΔCBM) were expressed in *Pichia pastoris*, and their characteristics were comprehensively compared. In addition, their hydrolytic action alone or combined with xylanase and cellulase on free-XG, complex substrates (xyloglucan-coated phosphoric acid swollen cellulose) and different pretreated natural xyloglucan-rich biomasses (corn bran and apple pomace) were also investigated.

Results And Discussion

Expression and purification of TtGH74 and TtGH74ΔCBM

The codon-optimized genes encoding GH74 xyloglucanase from *T. terrestris* (*Tt*GH74) and CBM-deleted variant *Tt*GH74ΔCBM were successfully expressed in *P. pastoris* KM71H. The purified enzymes were analyzed by SDS-PAGE with molecular masses of about 90 kDa and 85 kDa, respectively. After digestion with N-glycosidase Endo H, SDS-PAGE analysis showed that the molecular masses of *Tt*GH74 and *Tt*GH74ΔCBM decreased closely to their theoretical values of 87.89 kDa and 83.09 kDa, respectively (Fig. 1) The analysis of amino sequence of *Tt*GH74 by NetNGlyc 1.0 Server (https://services.healthtech.dtu.dk/service.php?NetNGlyc-1.0) confirmed that it has three putative N-glycosylation sites (N212, N325 and N409), indicating that the recombinant *Tt*GH74 and *Tt*GH74ΔCBM could partially be N-glycosylated.

Optimization of TtGH74 expression conditions

The protein expression level of *Tt*GH74 was only 60% of that of *Tt*GH74ΔCBM, therefore, the expression conditions of *Tt*GH74 were optimized. Methanol-regulated promoter of the alcohol oxidase 1 gene (AOX1) is the key to the high expression levels of recombinant protein in *P. pastoris* (35), which was significantly influenced by methanol concentration. In addition, the expression level was also affected by medium pH, induction temperature and time.

The optimum culture temperature for production of *Tt*GH74 was 28 ℃ (Fig. S4 a). As shown in Fig. S4 b, the optimal methanol concentration was observed at 1.5% (vol/vol), excessive methanol decreased the expression of *Tt*GH74 in *P. pastoris*. The optimum induction pH was pH 6.0 (Fig. S4 c). Under the optimized condition, the enzyme activity of *Tt*GH74 secreted in the supernatant reached to 95 U/mL after 5 days of induction with 1.5% methanol at pH 6.0 and 28 ℃ (Fig. S4 d).

Properties of recombinant TtGH74 and TtGH74ΔCBM from P. pastoris

Among all tested substrates, *Tt*GH74 showed an ultra-high activity against tamarind seed XG. *Tt*GH74 also showed activities toward barley β-glucan, konjac glucomannan, lichenan, and PASC, but the corresponding activities were only approximately 5% and 1% of that on xyloglucan. No activities were detected towards other polysaccharides such as laminarin, starch, xylan, pectin, and chitin, etc (Table 1).

Table 1
Substrate specificity of *Tt*GH74

Substrate	Glycosidic bond	*Tt*GH74 activity
β-Glucan (barley)	β-1,3 and β-1,4	++
Glucomannan (konjac)	β-1,4	++
Lichenan (lichen of iceland)	β-1,3 and β-1,4	+
Xyloglucan (tamarind seed)	β-1,4 α-1,6 and β-1,6	+++++
Laminarin (laminaria)	β-1,6-endo-β-1,3	
Soluble starch (potato)	α-1,4	
Xylan (birch)	β-1,4	
Arabinoxylan (wheat)	β-1,4	
Pectin	α-1,4	
Chitin	β-1,4	
CMC-Na	β-1,4	
Avicel	β-1,4	
Phosphoric acid swelling cellulose (PASC)	β-1,4	+

*Tt*GH74 and *Tt*GH74ΔCBM displayed the maximum activity toward tamarind seed XG at 75 ℃ and pH 5.5 (Fig. 2a, b). However, the enzymes were unstable at 70 ℃, after pre-incubation with 70 ℃ for 20 min, their residual activity was dropped to below 20% (Fig. 2c). This result indicated that the enzymes had more thermostability at presence of the substrate, which may be attributed to the stabilizing effects of substrate binding (36). Interestingly, the deletion of CBM1 significantly improved the thermostability of *Tt*GH74ΔCBM when pre-incubation of enzymes at temperature below 70 ℃. When preincubation of enzymes at 55 ℃ to 65 ℃ for 4 h, the residual activity of *Tt*GH74ΔCBM was 10–20% higher than that of *Tt*GH74. When the pre-incubation of enzymes at 50 ℃, the activity of *Tt*GH74 remained above 80%, while the activity of *Tt*GH74ΔCBM remained almost unchanged after 4 h of pre-incubation (Fig. 2c). Conversely, the thermostability of some glycoside hydrolases from fungi were decreased after the removal CBM1 (37, 38). The inconsistent observation about CBM1 suggested that its role in the thermostability of the enzyme might be related to the kind of enzymes. The enzyme was stable in the pH range from 3 to 8 (Fig. 2d).

The effect of metal ions (1 and 5 mM) on the enzymes activities was investigated and results are shown in Fig. S5. The activities of *Tt*GH74 and *Tt*GH74ΔCBM were increased by 2–25% in the presence of 5 mM K^+, Ca^{2+}, Ba^{2+} and Ni^{2+} ions. At the same time, the enzymes activities were decreased by 5%-75% in the presence of EDTA, NH_4^+, Li^+, Mg^{2+}, Pb^{2+}, Zn^{2+}, Cu^{2+}, Mn^{2+}, Co^{2+}, Fe^{3+} and Al^{3+} (1 and 5 mM). 5 mM Pb^{2+} and Fe^{3+} could dramatically reduce the enzyme activity, and the activities of *Tt*GH74 and *Tt*GH74ΔCBM were decreased by 90%.

The kinetic values were determined in the concentration ranges of 0.2-6 mg/mL of tamarind seed XG (Table 2). It can be seen from Table 2 that the catalytic activity of *Tt*GH74 is much higher than the previous characterized GH74 xyloglucanases. *Tt*GH74ΔCBM has slightly smaller K_m and K_{cat} value than *Tt*GH74 (Table 2). It was reported that

the K_{cat} of GH74 xyloglucanase from *Phanerochaete chrysosporium* was increased slightly after deletion of CBM1 (39). These results suggested that CBM1 in GH74 xyloglucanases did not significantly affect its catalytic activity for the soluble XG.

Table 2
Comparison of biochemical properties of *Tt*GH74 and *Tt*GH74ΔCBM with other GH74 xyloglucanases

Entry name	Strain	Temperature (°C)	pH	V_{max} (U/mg)	K_m (mg/mL)	K_{cat} (s^{-1})	References
*Tt*GH74	*Thielavia terrestris*	75	5.5	193.2	0.3225	283.36	This paper
*Tt*GH74ΔCBM				168.5	0.2671	233.09	
*Pc*GH74	*Phanerochaete chrysosporium*	55	6.0		0.25	28.1	(39)
*Pc*GH74ΔCBM					0.28	31.9	
*Mt*GH74	*Myceliophthora thermophila* VKPM	70–75	6.5		0.57		(40)
*Af*GH74	*Aspergillus fumigatus*	50	5.5	11.9	1.5	16.4	(41)
XEG74	*Paenibacillus sp* KM21	45	6.0	36.8	0.96	49.2	(42)
*Po*GH74	*Paenibacillus odorifer*	50	6.0		0.05	39.8	(43)

*Kcat: The number of moles of substrate that can be catalyzed per mole of enzyme per second.

The end-products generated from the tamarind seed XG after *Tt*GH74 hydrolysis were identified using matrix assisted laser desorption/ionization time-of-fight mass spectrometry (MALDI-TOF MS). A series of sodium adducts of hydrolyze products were detected. The m/z values of the major peaks were 1085, 1247 and 1409 corresponding to molecular masses of the reduced oligosaccharide ions $[XXXG + Na]^+$, $[XXLG + Na]^+$, and $[XLLG + Na]^+$, respectively. Besides the main XG building blocks, various low molecular products were generated during the hydrolysis, whose m/z values detected by mass spectrometry may potentially correspond to XX, XXG, GXX, XGX, XL, XLG, GXL, LL, LG, XXL, LLG, GXXXG, GXLLG, XLLGX oligosaccharides, respectively (Fig. 3). *Tt*GH74 released oligo-xyloglucans such as XXXG, XXLG, and XLLG which was the typical final products of *endo*-type xyloglucanases. In addition, the sequence alignments of *Tt*GH74 with other fungal GH74 xyloglucanases (Fig. S1) revealed that *Tt*GH74 have four conserved tryptophan residues which was regarded as the key amino acid residues for the *endo*-processive activity (26). Thus, indicated that *Tt*GH74 is *endo*-processive-type xyloglucanase.

Adsorption of TtGH74 and TtGH74ΔCBM on different substrates

The binding affinity of *Tt*GH74 and *Tt*GH74ΔCBM on different substrates (10 mg in 0.5 mL) was compared by measuring the unbound protein in the supernatant, the results are shown in Fig. 4a, all *Tt*GH74 protein bound onto PASC, while only approximately 35% and 23% of *Tt*GH74 bound onto Avicel and Whatman filter paper, respectively. For pretreated lignocellulosic substrates, the amount of bound protein in ascending order is 15%, 20% and 30% for deep eutectic solvents (DES) pretreated-corn bran, sulfuric acid pretreated-corn bran, and DES pretreated-apple pomace, respectively, directly proportional to the galactose content in the substrates (Table 3). Without CBM1, the adsorption capacity of *Tt*GH74ΔCBM for insoluble carbohydrates is almost completely lost. We further measured the adsorption of *Tt*GH74 under the condition of low cellulose content (1 mg in 0.5 mL) with additional different proportions of XG (Fig. 4b). Due to the relative excess amount of enzyme, the unbound protein was detected in supernatant, but as the increase of XG proportion, the amount of the unbound protein gradually decreased, which implied that the *Tt*GH74 could bind onto XG. To further verify the adsorption of CBM1 on XG, we compared the

mobility of CBM-deleted variant *Tt*GH74ΔCBM with the *Tt*GH74 in xyloglucan-containing native gels. It was observed that the mobility of *Tt*GH74ΔCBM was increased significantly compared to *Tt*GH74, which further clarified the binding affinity of CBM1 in *Tt*GH74 onto XG (Fig. 4c, d). The binding affinity of CBM1 on cellulose and role of CBM1 in cellulase functionality were well demonstrated in literatures (44, 45), CBM1 is type A CBM, and was previously recognized as cellulose-binding domain due to first discovery from fungal cellulases (3, 46). However, the effects of CBM1 on XG binding and activity of fungal GH74 xyloglucanases were few reported. Our results suggested that CBM1 in *Tt*GH74 displayed high binding affinity for both of cellulose and XG.

Hydrolysis action of TtGH74 and TtGH74ΔCBM on XG and XG-coated PASC

Hydrolysis action of *Tt*GH74 and *Tt*GH74ΔCBM on free XG was performed in the concentration ranges of 25–600 μg XG (Fig. 5a). When the amount of XG is low (less than 250 μg), *Tt*GH74ΔCBM exhibited a slightly lower hydrolysis yield than the intact enzyme due to its low affinity to the substrate. However, as the amount of XG increased, the yield of reducing sugars by *Tt*GH74ΔCBM hydrolysis increased significantly, and surpassed the yield by *Tt*GH74 as the content of XG was over 250 μg.

XG-coated PASC with different proportions of XG were used as substrate to investigate the influence of CBM1 in enzyme functionality. XG can coat onto the surface of PASC once mixture, however, the association pattern between XG with PASC relies on the proportion ratio of XG/PASC. The previous researches revealed that at low XG/cellulose concentration ratio (25 μg/mg), all XG are tightly bound to the cellulose surface, and XG is not easy to be hydrolyzed by enzyme. However, with the increase of XG/cellulose ratio, XG forms accessible “loops” and “tails” on the cellulose surface, and the accessible XG gradually increases to a constant value (47). The schematic diagram of the association pattern of XG and PASC is shown in Fig. 5b.

When XG-coated PASC was reacted with *Tt*GH74 or *Tt*GH74ΔCBM (Fig. 5a), XG was more difficult to be hydrolyzed than free XG by *Tt*GH74 and *Tt*GH74ΔCBM because of the close association of XG with PASC. Similar as free XG, once the proportion of XG increased over 400 μg/mg, *Tt*GH74ΔCBM released more reducing sugars from XG-coated PASC than *Tt*GH74. The free XG was detected in the supernatant of XG/PASC solution once the ratio was greater than 400 μg/mg, so the higher catalytic performance of *Tt*GH74ΔCBM than *Tt*GH74 in the hydrolysis of XG-coated PASC solution as the proportion of XG over 400 μg/mg might be due to the presence of free XG in solution. However, it was worth noted that a relative higher reducing sugars were released from XG-coated PASC by *Tt*GH74 than *Tt*GH74ΔCBM as the proportion ratio of XG/PASC below 300 μg/mg. These results indicated that CBM1 might not be essential for hydrolysis of free XG, but effective for the associated XG to some degree. The coverage of XG on PASC even at low concentration also resulted in a significant decrease in the catalytic activity of EG1, in comparison, a less decrease in CBH1 activity was observed. These differences might be attributed to the different catalytic pattern between EG1 and CBH1. EG1 is a GH5 *endo*-glucanase which randomly attacks on internal sites in the cellulose chain (48), while CBH1 is an *exo*-cellulase which processively hydrolyzes the cellulose chain from reducing end (49).

Hydrolysis action of TtGH74 or TtGH74ΔCBM on pretreated corn bran and apple pomace

Corn bran and apple pomace were chosen as enzymatic substrates. The product yield was expressed in grams of reducing sugar produced by per kilogram of dry material (Reducing Sugars g/kg Dry Material, RS g/kg DM). Two substrates were pre-treated at 90 °C by 1% sulfuric acid or DES for different times (3, 6, 9, 12 h). Interestingly, no matter what kind of pretreatment methods and times used, *Tt*GH74 produced more reducing sugars than *Tt*GH74ΔCBM from pretreated corn bran after four days of reaction, while *Tt*GH74ΔCBM has better hydrolysis

performance on DES-pretreated apple pomace than *Tt*GH74 (Fig. 6). Finally, corn bran pretreated with sulfuric acid for 6 h, corn bran and apple pomace pretreated with DES for 9 h were used as substrates for further exploration. As shown in Table 3, three pretreated substrates differed in chemical compositions due to different sources and pretreatment methods. DES pretreatment was more effective in removal of lignin and hemicelluloses than sulfuric acid pretreatment for corn bran. DES pretreated-apple pomace had the highest content of galactose among three substrates. Galactose is a specific substituent in the side branch of XG. Galactose may also come from the main chain of residual pectin, but galactose in pectin of apple accounts for approximately 1% of total pectin according to the literature (50), so the galactose in pretreated apple pomace mainly comes from the side chain of XG. Therefore, the higher content of galactose represents the higher amount of XG in lignocelluloses. This may explain the higher adsorption capacity of *Tt*GH74 on DES pretreated-apple pomace than DES pretreated- and sulfuric acid pretreated-corn bran (Fig. 4a). This may also explain the much higher reducing sugars released from DES pretreated-apple pomace by either *Tt*GH74 or *Tt*GH74ΔCBM (Fig. 6c). It was worthy noted that the content of lignin in DES pretreated-corn bran is much lower than sulfuric acid pretreated-corn bran. This might contribute to the more reducing sugars generated from DES pretreated-corn bran than sulfuric acid pretreated-corn bran, although the content of XG is relatively lower in DES pretreated-corn bran (Fig. 6a, b).

Table 3
Chemical composition of pretreated corn bran and apple pomace substrates

	Lignin	Glucose	Xylose	Galactose	Mannose	Arabinose
Sulfuric acid pretreated-corn bran	20.73%	66.04%	8.10%	0.18%	1.82%	0.74%
DES pretreated-corn bran	11.10%	70.04%	7.78%	0.09%	0.98%	0.43%
DES pretreated-apple pomace	21.69%	43.22%	8.43%	2.59%	2.34%	0.22%

The presence of XG in three pretreated substrates was also confirmed by analyzing the *Tt*GH74 hydrolysis end-products using high performance anion exchange chromatography with pulsed amperometric detection (HPAEC-PAD) and MALDI-TOF MS. The various sodium adducts of oligosaccharides were released from sulfuric acid pretreated-corn bran, DES pretreated-corn bran and DES pretreated-apple pomace after *Tt*GH74 hydrolysis (Fig. 7). Some of the detected m/z values may correspond to XG, XX, LG, XXG, XGX, XL, GGL, XLG, GXL, XXL, XXXG, LLG, XXLG, GXXXG oligosaccharides, respectively. However, different pretreatment methods might have various fractionalization and modification effects on XG in lignocellulosic biomass. Therefore, the content change and structural modification of XG in different pretreated lignocellulosic biomasses resulted in different end product profiles in hydrolysates. The more amount of GGL, XLG and GXL oligosaccharides were released from sulfuric acid pretreated-corn bran, while more XX, LG, XL, XXG, XGX oligosaccharides were released from either DES pretreated corn bran or apple pomace.

Time course of enzymatic hydrolysis of three pretreated substrates in different concentrations (from 10 to 80 mg) was performed and results are shown in Fig. 8. In general, *Tt*GH74 produced more reducing sugars than *Tt*GH74ΔCBM from sulfuric acid-pretreated corn bran and DES-pretreated corn bran after four days of hydrolysis, but the increase ranges varied depended on the concentration of substrates. For the two pretreated corn brans, at low substrate concentration (10 mg), the yield of reducing sugar by *Tt*GH74 was 1.23 and 1.39 times higher than *Tt*GH74ΔCBM. The yield of reducing sugar by *Tt*GH74 was 1.36 and 1.13 times higher than *Tt*GH74ΔCBM when the substrate concentration was 20 mg. While at concentrations of 40–80 mg, the yield of reducing sugar by *Tt*GH74 was about 1.12 times higher than that of *Tt*GH74ΔCBM. On the contrary, *Tt*GH74ΔCBM produced more reducing

sugars than *Tt*GH74 from DES-pretreated apple pomace, no matter what concentration of substrate was used. The yield of reducing sugar by *Tt*GH74ΔCBM was 1.68–2.06 times higher than that of *Tt*GH74 at concentrations of 10–80 mg. From the time course experiment, it could be concluded that the presence of CBM1 is conducive to enzymatic hydrolysis, but its role and significance are substrate-specific because of the differences in the contents and structure of XG in different biomasses.

Synergistic action of TtGH74 or TtGH74ΔCBM with CBH1/EG1 mixture and xylanase on pretreated corn bran and apple pomace

As specific xyloglucan degrading enzymes, GH74 xyloglucanases were widely distributed in bacteria and fungi, and usually were co-expressed with cellulase and xylanase. In view of the presence of XG in pretreated corn bran and apple pomace (Table 3) and its blocking effect on EG1 and CBH1 activity towards XG-coated PASC (Fig. 5), it is reasonable to believe that xyloglucanases may be necessary for efficient enzymatic saccharification of XG-rich biomasses. So, we further investigated the synergy between xyloglucanase, xylanase and cellulase in hydrolysis of pretreated corn bran and apple pomace. As shown in Fig. 9 (a, b), the reducing sugar yields of *Tt*GH74 hydrolysis were 13.88, 17.74, 13.97 (RS g/kg DM) for sulfuric acid pretreated-corn bran, DES pretreated-corn bran and DES pretreated-apple pomace, respectively, while the reducing sugar yield of GH10 xylanase hydrolysis were 16.54, 10.94, 5.22, respectively, and the reducing sugar yield of CBH1/EG1 mixture hydrolysis were 81.41, 70.26, 23.94, respectively. Correspondingly, when the enzymes acting synergistically, the yield of the combined action of GH10 xylanase with CBH1/EG1 mixture were 131.38, 96.70, 27.72, respectively, and the degree of synergy was 1.34, 1.19 and 0.95, respectively. The yield of the combined action of *Tt*GH74 with CBH1/EG1 mixture were 192.30, 119.84, 47.08, and the degree of synergy reached up to 2.02, 1.36 and 1.24, respectively. Furthermore, the yield of the combined action of *Tt*GH74, GH10 xylanase and CBH1/EG1 mixture were 241.25, 152.83, 77.19, and the degree of synergy was 2.16, 1.54 and 1.79 for sulfuric acid pretreated-corn bran, DES pretreated-corn bran and DES pretreated-apple pomace, respectively. The above results indicated that either *Tt*GH74 or GH10 xylanase showed boosting effect on the hydrolysis efficiency of CBH1/EG1 mixture, in comparison, the synergistic action between *Tt*GH74 and the CBH1/EG1 mixture was significantly higher than that of GH 10 xylanase and CBH1/EG1 mixture. Interesting, the degree of synergy between GH10 xylanase and *Tt*GH74 was 0.62, 0.88 and 0.69, respectively, indicating that GH10 xylanase and *Tt*GH74 not only had no synergy, but also had inhibition effect on each other due to the close spatial location of xyloglucan and xylan. However, the quaternary mixture of *Tt*GH74, GH10 xylanase and CBH1/EG1 resulted in more synergistic action than ternary mixture of *Tt*GH74 with CBH1/EG1.

For three pretreated substrates, when replacing *Tt*GH74 with *Tt*GH74ΔCBM in the enzymatic hydrolysis, the reducing sugar yield of *Tt*GH74ΔCBM hydrolysis were 9.54, 16.00, 23.30 (RS g/kg DM) for sulfuric acid pretreated-corn bran, DES pretreated-corn bran and DES pretreated-apple pomace, respectively. The yield of the combined action of *Tt*GH74ΔCBM with CBH1/EG1 mixture were 121.20, 105.39, 65.06, and the degree of synergy was 1.33, 1.22 and 1.38, respectively. The yield of the combined action of *Tt*GH74ΔCBM with GH10 xylanase and CBH1/EG1 mixture were 195.42, 145.68, 98.80, and the degree of synergy reached up to 1.82, 1.50, 1.88, respectively. Similarly, no synergy but inhibition effect on each other was observed for *Tt*GH74ΔCBM and GH10 xylanase, and the degree of synergy was 0.60, 0.82 and 0.44, respectively.

It can be inferred from the above results, the addition of *Tt*GH74 or *Tt*GH74ΔCBM into the CBH1/EG1 mixture or quaternary mixture of CBH1/EG and GH10 xylanase facilitated the overall hydrolysis of three pretreated substrates. The boosting effect of *Tt*GH74 in CBH1/EG1 mixture or quaternary mixture of CBH1/EG and GH10 xylanase was relatively higher than *Tt*GH74ΔCBM in terms of the degrees of synergy for sulfuric acid pretreated-corn bran (2.02

and 1.36 vs 1.33 and 1.22) and DES pretreated-corn bran (2.16 and 1.54 vs 1.82 and 1.50). In contrast, the boosting effect of *Tt*GH74ΔCBM was much higher than *Tt*GH74 in terms of the degree of synergy for pretreated apple pomace (1.38 and 1.88 vs 1.24 and 1.79). This is consistent with the bias of their activities when acted on three pretreated substrates alone, i.e. *Tt*GH74 showed higher activity towards pretreated corn bran than *Tt*GH74ΔCBM, conversely, *Tt*GH74ΔCBM had much higher activity than *Tt*GH74 towards pretreated apple pomace (Fig. 8).

In order to verify whether the above synergistic action between xyloglucanase and other glycoside hydrolases was attributed to the presence of XG in the substrates, the associated XG was extracted by strong alkali treatment and XG-free residuals were used as substrates for synergistic experiments. As shown in Fig. S6, no oligosaccharides could be released from strong alkali treated-residual by *Tt*GH74 hydrolysis based on the analysis of HPAEC-PAD, indicating that that strong alkali treated-residual did not contain XG. In addition, almost no reducing sugar was produced from strong alkali treated-residual by GH10 xylanase hydrolysis (Fig. 9c), indicating that the strong alkali treatment also removed xylan from pretreated-lignocellulose. When XG-free substrates were hydrolyzed by the mixture of CBH1/EG1 and GH10 xylanase, CBH1/EG1 and *Tt*GH74, and the mixture of *Tt*GH74, CBH1/EG1 and GH10 xylanase, no synergistic action was observed. Their corresponding reducing sugar yields were almost as same as that of CBH1/EG1 mixture alone, and all degrees of synergy were close to 1, (Fig. 9c, d). However, we found that the hydrolysis efficiency of CBH1/EG1 mixture on the strong alkali treated residues was greatly improved. The reducing sugar yields reached up to 192.29, 114.81 and 93.54 (RS g/kg DM), respectively, which were 136.20%, 63.41% and 290.72% higher than the corresponding reducing sugar yields of CBH1/EG1 mixture on sulfuric acid pretreated-corn bran, DES pretreated-corn bran and DES pretreated-apple pomace, respectively (Fig. 9a). Thus, further confirmed that the blocks of XG is one of great significance factors impeding the degradation of xyloglucan-rich lignocellulose.

The structures, activity modes and enzymatic properties of GH74 xyloglucanases have been widely studied in literatures (26, 27, 39–43), but their roles in lignocellulose biomass degradation has been rarely reported, Benko et al.(18) studied the contribution of the added GH74 xyloglucanase from *Trichoderma reesei* (*Tr*GH74) in the cellulase mixture to degradation of willow, barley straw, wheat straw, reed canary grass, corn stover and Solka Floc. It was found that the degree of synergy of *Tr*GH74 with the cellulase mixture reached to 1.22 for barley straw, but only 1.07 and 1.10 for corn stover, and reed canary grass and willow, respectively. No synergistic effect was observed for wheat straw and Solka Floc. It was suggested that the degree of synergy was positively correlated with the content of XG in the substrate. Corn bran (or corn fibre) is an agricultural by-product obtained from corn processing. It was well recognized that corn bran polysaccharides were very difficult to be decomposed by enzymatic hydrolysis (51–54). Its recalcitrance was regarded due to the rich content of glucuronoarabinoxylan which was extensively decorated with variations of both monomeric and oligomeric substitutions (55). Apple pomace is the by-product from apple processing rich in pectin, cellulose and hemicelluloses (56), and could be a raw material for biofuel and biochemical production (57); however, the enzymatic saccharification of apple pomace has not well investigated. In this study, we demonstrated that both of them have rich in xyloglucan which was closely associated with other polysaccharides and still remained in solid residues after pretreatment. The associated XG significantly hindered the enzymatic hydrolysis efficiency. Our results demonstrated that the hydrolysis performance of cellulase mixture on pretreated XG-rich biomasses could be greatly improved by adding the so-called accessory enzyme xyloglucanase to enzyme mixture.

Conclusions

In this study, we characterized and comprehensively compared *Tt*GH74 and *Tt*GH74ΔCBM from *T. terrestris*. Deletion of CBM1 improved the thermostability, but decreased K_{cat} slightly, and was almost completely lost its adsorption capacity for insoluble carbohydrates. We also compared the hydrolysis of free XG, XG-coated PASC, pretreated corn bran and apple pomace by *Tt*GH74 or *Tt*GH74ΔCBM action alone or combined with other glycoside hydrolases. The results showed that CBM1 might not be essential for hydrolysis of free XG, but effective for the associated XG to some extent. *Tt*GH74 could remove the bound xyloglucan on cellulose, therefore efficiently boosted the enzymatic hydrolysis of the pretreated XG-rich lignocellulosic biomass. The presence of CBM1 is conducive to enzymatic hydrolysis, but its role and significance is substrate-specific due to the differences of XG contents in various biomasses. This study deepened our understanding about the effect of CBM1 on the enzymatic properties of GH74 xyloglucanases and the roles of enzyme in the degradation of different XG-rich biomasses.

Materials And Methods

Materials

Chemicals and reagents used in this study were analytical grade. Xyloglucan (tamarind seed), β-glucan (barley), glucomannan (konjac), lichenan (lichen of iceland), arabinoxylan (wheat) were purchased from Megazyme (Ireland); laminarin (laminaria), xylan (birch), pectin, sodium hydroxymethylcellulose (CMC-Na) and Avicel were purchased from Sigma Aldrich (Shanghai, China); soluble starch (potato) and chitin were obtained from Sangon (Shanghai, China); phosphoric acid swollen cellulose (PASC) was prepared from Avicel according to the protocol described by Zhang et al (58). Whatman filter paper was provided from Maidstone England.

Corn bran was collected from Nanyang, Henan Province, China. Destarched corn bran was prepared by amylase and papain treatment according to the method used by Rose and Inglett (59) with modifications. Amylase and papain were purchased from Imperial Jade Bio-Technology Co., Ltd. (Ningxia, China). Apple pomace was purchased from Yuanzhi Biotechnology Co., Ltd (Shaanxi, China). The destarched corn bran was pretreated either with 1 % sulfuric acid or deep eutectic solvents (DES, lactic acid: ChCl molar ratio was 2:1). Apple pomace was also pretreated with DES as same solution for destarched corn bran. The pretreatment temperature was 90 ℃ and reaction times were 3, 6, 9 and 12 h, respectively. After pretreatment, the residues were washed with distilled water to neutral and dried at 105 ℃ to a constant weight. Finally, corn bran pretreated with sulfuric acid for 6 h, corn bran and apple pomace pretreated with DES for 9 h were used as substrates for further exploration. In order to verify whether XG exists in three pretreated substrates, the substrates were hydrolyzed by *Tt*GH74 in the 1 mL reaction mixture containing 20.7 nM of *Tt*GH74 (15 U/g substrate), and 20 mg substrate in 50 mM sodium acetate buffer (pH 5.5) in the shaking incubator at 50 ℃ and 200 rpm for 96 h. Then the end-products were analyzed by HPAEC-PAD and MALDI-TOF MS. The extraction of XG in above pretreated materials was carried out by using strong alkali according to literature (60). Briefly, the pretreated materials were soaked in 15 % NaOH at room temperature for 24 h, and then wash the strong alkali treated residues to neutral with distilled water and dried at 80 ℃ to a constant weight. In order to verify whether XG was retained in the strong alkali treated residues, the residues were hydrolyzed by *Tt*GH74 in same condition described above. And the released of oligosaccharides was analyzed by HPAEC-PAD.

Endoglucanase 1 (EG1) from *Volvariella volvacea* and GH10 xylanase from *Eupenicillium parvum* 4–14 were expressed in *Pichia pastoris* KM71H according to previous methods (48, 61), and cellobiohydrolase 1 (CBH1) from *Hypocrea jecorina* was purchased from Sigma-Aldrich (Shanghai, China).

Construction of *Tt*GH74 and *Tt*GH74ΔCBM

A gene fragment encoding mature xyloglucanase from *T. terrestris* NRRL 8126 (*Tt*GH74, XP_003650520.1) was synthesized by GenScript (Nanjing, China) with modified codons according to the codon preference of *P. pastoris*. The gene fragment was linked to the pPICZαA expression vector (Invitrogen, Carlsbad, CA, USA), located between *Eco*RI and *Not*I sites. The CBM1 fragment in *Tt*GH74 was removed by PCR using the following primers (Table 4).

Table 4 Primers used in this study

Primer	Sequence (5' to 3')
5'AOX	GACTGGTTCCAATTGACAAG
*Tt*GH74ΔCBM-R	ATAGTTTAGCGGCCGCTTAGTGATGGTGATGGTGATGGTGAGATTGAGTAGCTTGAGG

The phylogenetic tree was created using the software MEGA (version 7), the method is neighbor-joining. The sequences encoding signal peptide, linker peptide, and CBM in selected genes were deleted, and only the catalytic domain (CD) was selected for sequence alignment. Structural models of *Tt*GH74 were generated with SWISS-MODEL (http://swissmodel.expasy.org/). The 3D protein structure images of CD and CBM1 of *Tt*GH74 were generated with PyMOL version 2.2.0 (Schrodinger LLC, New York, NY, USA).

Expression and purification of *Tt*GH74 and *Tt*GH74ΔCBM

Linearized by the restriction enzyme *Sac*I, the recombinant plasmids were integrated into the genome of *P. pastoris* KM71H host cells by electroporation. Transformed colonies were picked from yeast extract-peptone-dextrose medium containing 0.1% zeocin (YPDZ) to 100 mL buffered complex glycerol (BMGY) medium (100 mM potassium phosphate, pH 6.0, 1.34% (w/v) yeast nitrogen base (YNB), 1% yeast extract, 2% peptone, and 1% glycerol) in a shaking incubator (200 rpm) at 28 ℃ until the culture reached an OD600 of 3. The cells were harvested by centrifugation at 4000 rpm for 5 min and then decanted to 50 mL buffered methanol complex (BMMY) medium (100 mM potassium phosphate, pH 6.0, 1.34% (w/v) YNB, 1% yeast extract, 2% peptone). To induce expression, methanol was added to a final concentration of 1 % every 24 h. After 7 days, the culture was centrifuged (10000 rpm, 10 min) and the supernatant was then directly loaded to the Ni-NTA pre-packed gravity column (Sangon Biotech, Shanghai, China). The purification steps were performed according to the manufacturer's manual. The purified enzyme was dialyzed at 4 ℃ for 12 h to exclude imidazole. The protein was quantified using a Pierce BCA Protein Assay kit (Thermo Fisher, Rockford, USA). Polyacrylamide (12.5 %) gel electrophoresis in 0.1 % SDS was carried out to determine the molecular mass of the enzyme preparation. Proteins were visualized after staining with Coomassie Brilliant Blue R-250.

The deglycosylation of the recombinant protein was performed by treating the protein with Endoglycosidase H (Endo H, endo-N-acetylglucosaminidase H of *Streptomyces plicatus*; NEB, Ipswich, MA, USA) according to the manufacturer's instructions.

Optimization of *Tt*GH74 expression conditions

For optimizing expression of *Tt*GH74, the effects of temperature (24 ℃, 26 ℃, 28 ℃, 30 ℃ and 32 ℃), methanol concentration (0.5 % to 2.0 %), pH (5.0, 6.0 and 7.0), and induction time (1 to 7 days) on the *Tt*GH74 expression were investigated step by step. For methanol concentration optimization, the pH was kept at 6.0, whereas for pH optimization, the methanol concentration was maintained at 1.5 %, respectively. The culture temperature was 28 ℃.

Properties of recombinant *Tt*GH74 and *Tt*GH74ΔCBM from *P. pastoris*

The enzyme activity on tamarind seed XG was measured in 0.5 mL reaction mixture containing 2 mg XG, 10 nM *Tt*GH74 or *Tt*GH74ΔCBM in 50 mM sodium acetate buffer (pH 5.5) at 75 ℃ for 15 min. The amount of reducing sugars released from the substrate was determined by using 3,5-dinitrosalicylic acid reagent (DNS) method (62). One unit of enzyme activity was defined as the amount of enzyme that catalyzed the conversion of substrate to 1 μmol of glucose equivalent per minute. To determine the substrate specificity of *Tt*GH74, the following polysaccharides were selected: tamarind seed XG, β-glucan, glucomannan, lichenan, arabinoxylan, laminarin, xylan, pectin, CMC-Na, soluble starch, chitin, avicel, and PASC. The reaction was performed at same assay condition described above instead of individual selected substrate was used. The end products generated from tamarind seed XG by the *Tt*GH74 hydrolysis were analyzed using MALDI-TOF MS.

The optimal temperatures and pHs, thermal and pH stability of *Tt*GH74 and *Tt*GH74ΔCBM were measured on tamarind seed XG. Optimum temperatures were determined at a range of temperature from 35 to 85 ℃. Optimal pHs were determined in buffers in a range of pH 3.5-8.0 (50 mM sodium acetate buffer (pH 3.5-6.0), 50 mM sodium phosphate buffer (pH 6.0 - 8.0)). The maximum enzyme activity was taken as 100 % and relative activities were calculated. Thermostability of the enzymes was determined by pre-incubating the recombinant enzymes at 50 to 70 ℃ for a specific time and the residual enzyme activities were determined at assay condition. The activity of *Tt*GH74 and *Tt*GH74ΔCBM before incubation was taken as 100 % and the relative activities were calculated. The pH stability was tested by preincubation of the recombinant enzyme in 50 mM buffer at various pH values (3.0–8.0) at 4 ℃ overnight, and the residual enzyme activities were measured as above. To investigate the effect of metal ions on *Tt*GH74 and *Tt*GH74ΔCBM activities, the enzymes activities were assayed at presence of 1 mM or 5 mM metal ions (Li^+, K^+, Mg^{2+}, Pb^{2+}, Ca^{2+}, Zn^{2+}, Ba^{2+}, Cu^{2+}, Ni^{2+}, Mn^{2+}, Co^{2+}, Fe^{3+}, Al^{3+}), NH^{4+} and EDTA, the reaction was carried out at 50 ℃ for 15 min. The K_m value against tamarind seed XG was determined at 50 ℃ for 7.5 min, using a substrate concentration in the ranges of 0.2– 6 mg/mL. The K_m and other kinetic values were calculated with the GraphPad Prism 8.0 program.

Adsorption of *Tt*GH74 and *Tt*GH74ΔCBM on different substrates

The adsorption of enzymes on different substrates was studied by incubating the *Tt*GH74 or *Tt*GH74ΔCBM in the mixture volume 0.5 mL with a final concentration of 300 μg/mL protein and 10mg substrate in 50 mM sodium acetate buffer (pH 5.5) at 0 °C for 1 h with shaking (100 rpm). The substrates were Whatman filter paper, Avicel, PASC, sulfuric acid pretreated-corn bran, DES pretreated-corn bran and DES pretreated-apple pomace. After the incubation, the mixture was centrifuged at 10000 rpm for 10 min. The unbound protein in supernatant was quantified using a Pierce BCA Protein Assay kit. The adsorption of *Tt*GH74 on XG coated PASC was determined at the same incubation condition. The 0.5 mL mixture containing a final concentration of 300 μg/mL protein and 1mg PASC with different proportion of XG. The XG coated PASC was prepared by premixing an aqueous solution of XG (0 to 600 (μg/mg)) with 1mg PASC at room temperature in total 0.5 mL of 50 mM sodium acetate buffer (pH 5.5) with stirring (rotary disc contactor, 20 rpm) for 18 h (47). Difference in binding affinity between *Tt*GH74 and *Tt*GH74ΔCBM to XG was determined by affinity electrophoresis (AE). AE was carried out in 7.5% polyacrylamide gels containing 0.005 w/v soluble XG at 0 ℃ and 150 V for 3 h (63).

Hydrolysis action of *Tt*GH74 and *Tt*GH74ΔCBM on XG and XG-coated PASC

Hydrolysis action of *Tt*GH74 or *Tt*GH74ΔCBM on free XG was performed in the reaction mixture 0.5 mL containing 10 nM *Tt*GH74 or *Tt*GH74ΔCBM, and different amounts (25-600 μg) of XG in 50 mM sodium acetate buffer (pH 5.5)

in the shaking incubator at 50 °C and 200 rpm for 1 h. Then the amount of reducing sugar was detected by DNS method. Hydrolysis action of *Tt*GH74 or *Tt*GH74ΔCBM on XG-coated PASC was performed in same reaction condition but using XG-coated PASC as substrate. The hydrolytic activity of EG1 or CBH1 towards XG-coated PASC was also performed in same reaction condition but with 2.5 μg EG1 or 2.5 μg CBH1, respectively. In order to determine the free XG in XG-coated PASC solution, the liquid fraction was separated by centrifugation and the unbound XG in the supernatant was completely hydrolyzed by *Tt*GH74, and reducing sugars was measured by DNS method.

Hydrolysis action of *Tt*GH74 or *Tt*GH74ΔCBM on pretreated lignocellulose

Hydrolysis action of *Tt*GH74 or *Tt*GH74ΔCBM on pretreated lignocelluloses (sulfuric acid pretreated-corn bran, DES pretreated-corn bran and DES pretreated-apple pomace) with different pretreatment times was performed in the 1 mL reaction mixture containing 20.7 nM of *Tt*GH74 or *Tt*GH74ΔCBM (15 U/g substrate), and 20 mg substrate in 50 mM sodium acetate buffer (pH 5.5) in the shaking incubator at 50 °C and 200 rpm for 96 h, and 0.1 % antibiotics (zeocin and ampicillin) were added to the reaction mixture to prevent product degradation. The reducing sugars produced after hydrolysis were detected by DNS method.

Time course of enzymatic hydrolysis of three pretreated substrates (corn bran pretreated with sulfuric acid for 6 h, corn bran and apple pomace pretreated with DES for 9 h) in different concentrations (from 10 to 80 mg) was performed by *Tt*GH74 or *Tt*GH74ΔCBM in same condition described above. Samples were taken out every 12 h and the reducing sugars produced after hydrolysis were detected by DNS method.

Synergistic action of *Tt*GH74 or *Tt*GH74ΔCBM with CBH1/EG1 mixture and xylanase on pretreated lignocellulose

The synergy of *Tt*GH74 or *Tt*GH74ΔCBM with cellulase and xylanase on pretreated lignocellulose were performed by mixed action of *Tt*GH74 or *Tt*GH74ΔCBM with GH10 xylanase, CBH1/EG1 mixture, and GH10 xylanase and CBH1/EG1 mixture, respectively. The synergy of GH10 xylanase with CBH1/EG1 mixture on pretreated lignocellulose were also performed by mixed action GH10 xylanase with CBH1/EG1 in same condition. The dosage of each enzyme was as follows: 20.7 nM of *Tt*GH74 or *Tt*GH74ΔCBM (15 U/g substrate), 15 U/g substrate of GH10 xylanase, 25 μg EG1 and 25 μg CBH1 for pretreated corn bran; while the dosage of each EG1 and CBH1 was reduced to 15 μg for DES pretreated apple pomace because the cellulose content in DES pretreated-apple pomace is only about 60 % of that in DES pretreated-corn bran. The synergistic action was conducted in a shaking incubator at 50 °C and 200 rpm for 96 h, and the volume of reaction mixture was 1 mL containing 20 mg substrate and appropriate enzymes in the 50 mM sodium acetate buffer (pH 5.5) with 0.1 % antibiotics. The reducing sugars produced after hydrolysis were detected by DNS method.

The degree of synergy (DS) of the coupled enzyme mixture was calculated by Eq.1.

$$DS=\frac{RS_{total}}{RS_{enzyme\ 1}+RS_{enzyme\ 2}+RS_{enzyme\ 3}+\cdots} \quad (1)$$

where RS_{total} is the reducing sugar released by enzymes when used together, and the denominator is the sum of the yield of reducing sugars when the enzymes are used separately in the same amounts as they were employed in the mixture.

In addition, the synergy of *Tt*GH74 with cellulase and xylanase on alkali treated residues of sulfuric acid pretreated-corn bran, DES pretreated-corn bran and DES pretreated-apple pomace were determined at the same reaction

conditions as described above. The reducing sugars produced after hydrolysis were detected by DNS method.

Test method

The chemical composition analysis of pretreated solid fractions (lignin, glucose, xylose, galactose, mannose and arabinose) was performed according to the analytical procedure provided by the National Renewable Energy Laboratory (NREL/TP-510-42618 (64)), and the carbohydrates in supernatant were then quantified by high performance liquid chromatography (HPLC) (Agilent, Palo Alto, CA, USA). The HPLC system fitted with a Bio-Rad Aminex HPX-87H column was operated at 55 °C with 5 mM H_2SO_4 as the mobile phase at the flow rate of 0.6 mL/min as previously described by Chen et al. (65). HPAEC-PAD analysis was performed on a Dionex ICS-5000 system (Dionex, Sunnyvale, CA, USA) equipped with pulsed amperometric detection (PAD) and a CarboPac PA200 analytical column (3 × 250 mm) with a CarboPac PA200 guard column (3 × 50 mm) according to Shi et al. described method (13). MALDI-TOF MS analysis was performed on a 5800 MALDI TOF/TOF analyzer (AB SCIEX, Foster City, CA, USA) equipped with a neodymium: yttrium-aluminum-garnet laser (laser wavelength was 349 nm) according to Shi et al. described method (13).

All described experiments were performed in triplicate and mean values were reported along with the standard deviations.

Availability of data and materials

All data generated or analyzed during this study are included in this manuscript and its additional file.

Abbreviations

GH74: Glycoside hydrolase family 74; CBM1: Family 1 carbohydrate binding module; *Tt*: *Thielavia terrestris*; XG: Xyloglucan; EG1: Endoglucanase 1; CBH1: Cellobiohydrolase 1; DES: Deep eutectic solvents; HPAEC-PAD: High performance anion exchange chromatography with pulsed amperometric detection; MALDI-TOF MS: Matrix assisted laser desorption/ionization time-of-fight mass spectrometry; HPLC: High-performance anion exchange chromatography.

Declarations

Acknowledgements

We thank the research Grant (No. 22178179) from the National Natural Science Foundation of China, and a Project funded by the Priority Academic Program Development of Jiangsu Higher Education Institutions, and the Doctorate Fellowship Foundation of Nanjing Forestry University.

Funding

This work was supported by a research Grant (No. 22178179) from the National Natural Science Foundation of China, and a Project funded by the Priority Academic Program Development of Jiangsu Higher Education Institutions, and the Doctorate Fellowship Foundation of Nanjing Forestry University.

Authors' contributions

BW researched and drafted the manuscript. LL, KC and PZ provided some experimental materials and guided the experimental process. SD designed and interpreted the experimental data and reviewed the manuscript. All authors read and approved the final manuscript.

Ethics approval and consent to participate

Not applicable.

Consent for publication

Not applicable.

Competing interests

The authors declare that they have no competing interests.

References

1. Huber GW, Iborra S, Corma A. Synthesis of transportation fuels from biomass: chemistry, catalysts and engineering. Chemical Reviews. 2006; 106:4044–4098. https://doi.org/10.1021/cr068360d
2. Sethupathy S, Morales GM, Li Y, Wang Y, Jiang J, Sun J, Zhu D. Harnessing microbial wealth for lignocellulose biomass valorization through secretomics: a review. Biotechnology for Biofuels. 2021; 14:154. https://doi.org/10.1186/s13068-021-02006-9
3. Pauly M, Keegstra K. Biosynthesis of the plant cell wall matrix polysaccharide xyloglucan. Annual Review of Plant Biology. 2016; 67:235–259. https://doi.org/10.1146/annurev-arplant-043015-112222
4. Chris S, Stefan B, Ginger B, Michelle F, Thorsten H, Jennifer M, Erin O, Alex P, Staffan P, Ted R, Sonja V, Heather Y. Toward a systems approach to understanding plant cell walls. Science. 2004; 306:2206–2211. https://doi.org/10.1126/science.1102765
5. Anna E. Structural diversity and application potential of hemicelluloses. Macromolecular Symposia. 2005; 232:1–12. https://doi.org/10.1002/masy.200551401
6. McNeil M, Darvill AG, Fry SC, Albersheim P. Structure and function of the primary cell walls of plants. Annual Review of Biochemistry. 1984; 53:625–663. https://doi.org/10.1146/annurev.bi.53.070184.003205
7. Fry SC. The structure and functions of xyloglucan. Journal of Experimental Botany. 1989; 40:1–11. https://doi.org/10.1093/jxb/40.1.1
8. Fry SC, York WS, Peter A, Alan D, Takahisa H, Jean-Paul J, Yoji K, Ester PL, Gordon AM, Michael MN, Andrew JM, JS GR, Hanns US, Robert RS, Alphons GJV, Alan RW. An unambiguous nomenclature for xyloglucan-derived oligosaccharides. Physiologia Plantarum. 1993; 89:1–3. https://doi.org/10.1111/j.1399-3054.1993.tb01778.x
9. Zabotina OA. Xyloglucan and its biosynthesis. Frontiers in Plant Science. 2012; 3:134. https://doi.org/10.3389/fpls.2012.00134
10. Ostby H, Hansen LD, Horn SJ, Eijsink VGH, Varnai A. Enzymatic processing of lignocellulosic biomass: principles, recent advances and perspectives. Journal of Industrial Microbiology & Biotechnology. 2020; 47:623–657. https://doi.org/10.1007/s10295-020-02301-8
11. Zoghlami A, Paes G. Lignocellulosic biomass: understanding recalcitrance and predicting hydrolysis. Frontiers in Chemistry. 2019; 7:874. https://doi.org/10.3389/fchem.2019.00874

12. Kothari N, Bhagia S, Pu Y, Yoo CG, Li M, Venketachalam S, Pattathil S, Kumar R, Cai CM, Hahn MG, Ragauskas AJ, Wyman CE. The effect of switchgrass plant cell wall properties on its deconstruction by thermochemical pretreatments coupled with fungal enzymatic hydrolysis or *Clostridium thermocellum* consolidated bioprocessing. Green Chemistry. 2020; 22:7924–7945.https://doi.org/10.1039/d0gc02546a
13. Shi YX, Chen KX, Long LK, Ding SJ. A highly xyloglucan active lytic polysaccharide monooxygenase EpLPMO9A from *Eupenicillium parvum* 4–14 shows boosting effect on hydrolysis of complex lignocellulosic substrates. International Journal of Biological Macromolecules. 2021; 167:202–213. https://doi.org/10.1016/j.ijbiomac.2020.11.177
14. Hori C, Gaskell J, Igarashi K, Samejima M, Hibbett D, Henrissat B, Cullen D. Genomewide analysis of polysaccharides degrading enzymes in 11 white- and brown-rot Polyporales provides insight into mechanisms of wood decay. Mycologia. 2013; 105:1412–1427. https://doi.org/10.3852/13-072
15. Borin GP, Sanchez CC, de Souza AP, de Santana ES, de Souza AT, Paes Leme AF, Squina FM, Buckeridge M, Goldman GH, Oliveira JV. Comparative secretome analysis of *Trichoderma reesei* and *Aspergillus niger* during growth on sugarcane biomass. PLoS One. 2015; 10:e0129275. https://doi.org/10.1371/journal.pone.0129275
16. Wang K, Zhang N, Pearce R, Yi S, Zhao X. Comparative secretomics analysis eeveals the major components of *Penicillium oxalicum* 16 and *Trichoderma reesei* RUT-C30. Microorganisms. 2021; 9:2042. https://doi.org/10.3390/microorganisms9102042
17. Hu JG, Arantes V, Pribowo A, Saddler JN. The synergistic action of accessory enzymes enhances the hydrolytic potential of a “cellulase mixture” but is highly substrate specific. Biotechnology for Biofuels. 2013; 6:112. https://doi.org/10.1186/1754-6834-6-112
18. Benko Z, Siika-aho M, Viikari L, Reczey K. Evaluation of the role of xyloglucanase in the enzymatic hydrolysis of lignocellulosic substrates. Enzyme and Microbial Technology. 2008; 43:109–114. https://doi.org/10.1016/j.enzmictec.2008.03.005
19. Hu JG, Arantes V, Saddler JN. The enhancement of enzymatic hydrolysis of lignocellulosic substrates by the addition of accessory enzymes such as xylanase: is it an additive or synergistic effect? Biotechnology for Biofuels. 2011; 4:36. https://doi.org/10.1186/1754-6834-4-36
20. Shimizu FL, de Azevedo GO, Coelho LF, Pagnocca FC, Brienzo M. Minimum lignin and xylan removal to improve cellulose accessibility. BioEnergy Research. 2020; 13:775–785. https://doi.org/10.1007/s12155-020-10120-z
21. Novy V, Nielsen F, Cullen D, Sabat G, Houtman CJ, Hunt CG. The characteristics of insoluble softwood substrates affect fungal morphology, secretome composition, and hydrolytic efficiency of enzymes produced by *Trichoderma reesei*. Biotechnology for Biofuels. 2021; 14:105. https://doi.org/10.1186/s13068-021-01955-5
22. von Freiesleben P, Spodsberg N, Stenbaek A, Stalbrand H, Krogh K, Meyer AS. Boosting of enzymatic softwood saccharification by fungal GH5 and GH26 endomannanases. Biotechnology for Biofuels. 2018; 11:194. https://doi.org/10.1186/s13068-018-1184-y
23. Pauly M, Andersen LN, Kauppinen S, Kofod LV, York WS, Albersheim P, Darvill A. A xyloglucan-specific endo-beta-1,4-glucanase from *Aspergillus aculeatus*: expression cloning in yeast, purification and characterization of the recombinant enzyme. Glycobiology. 1999; 9:93–100. https://doi.org/10.1093/glycob/9.1.93
24. Gusakov AV, Uporov IV, Sinitsyna OA. Molecular dynamics simulations of two GH74 endo-processive xyloglucanases and the mutated variants to understand better the mechanism of the enzyme action. Biochimica et Biophysica Acta-General Subjects. 2020; 1864:129721. https://doi.org/10.1016/j.bbagen.2020.129721

25. Matsuzawa T, Kameyama A, Nakamichi Y, Yaoi K. Identification and characterization of two xyloglucan-specific endo-1,4-glucanases in *Aspergillus oryzae*. Applied Microbiology and Biotechnology. 2020; 104:8761–8773. https://doi.org/10.1007/s00253-020-10883-7
26. Matsuzawa T, Yaoi K. GH74 xyloglucanases: structures and modes of activity. Trends in Glycoscience and Glycotechnology. 2016; 28:E63-E70. https://doi.org/10.4052/tigg.1510.1E
27. Arnal G, Stogios PJ, Asohan J, Atti MA, Skarina T, Viborg AH, Henrissat B, Savchenko A, Brumer H. Substrate specificity, regiospecificity, and processivity in glycoside hydrolase family 74. The Journal of Biological Chemistry. 2019; 294:13233–13247. https://doi.org/10.1074/jbc.RA119.009861
28. Gunnarsson LC, Dexlin L, Karlsson EN, Holst O, Ohlin M. Evolution of a carbohydrate binding module into a protein-specific binder. Biomolecular Engineering. 2006; 23:111–117. https://doi.org/10.1016/j.bioeng.2005.12.002
29. Abbott DW, van Bueren AL. Using structure to inform carbohydrate binding module function. Current Opinion in Structural Biology. 2014; 28:32–40. https://doi.org/10.1016/j.sbi.2014.07.004
30. Boraston AB, Bolam DN, Gilbert HJ, Davies GJ. Carbohydrate-binding modules: fine-tuning polysaccharide recognition. The Biochemical Journal. 2004; 382:769–781. https://doi.org/10.1042/BJ20040892
31. Inoue H, Kishishita S, Kumagai A, Kataoka M, Fujii T, Ishikawa K. Contribution of a family 1 carbohydrate-binding module in thermostable glycoside hydrolase 10 xylanase from *Talaromyces cellulolyticus* toward synergistic enzymatic hydrolysis of lignocellulose. Biotechnology for Biofuels. 2015; 8:77. https://doi.org/10.1186/s13068-015-0259-2
32. Bernardes A, Pellegrini VOA, Curtolo F, Camilo CM, Mello BL, Johns MA, Scott JL, Guimaraes FEC, Polikarpov I. Carbohydrate binding modules enhance cellulose enzymatic hydrolysis by increasing access of cellulases to the substrate. Carbohydrate Polymers. 2019; 211:57–68. https://doi.org/10.1016/j.carbpol.2019.01.108
33. Berka RM, Grigoriev IV, Otillar R, Salamov A, Grimwood J, Reid I, Ishmael N, John T, Darmond C, Moisan MC, Henrissat B, Coutinho PM, Lombard V, Natvig DO, Lindquist E, Schmutz J, Lucas S, Harris P, Powlowski J, Bellemare A, Taylor D, Butler G, de Vries RP, Allijn IE, van den Brink J, Ushinsky S, Storms R, Powell AJ, Paulsen IT, Elbourne LD, Baker SE, Magnuson J, Laboissiere S, Clutterbuck AJ, Martinez D, Wogulis M, de Leon AL, Rey MW, Tsang A. Comparative genomic analysis of the thermophilic biomass-degrading fungi *Myceliophthora thermophila* and *Thielavia terrestris*. Nature Biotechnology. 2011; 29:922–927. https://doi.org/10.1038/nbt.1976
34. Maheshwari R, Bharadwaj G, Bhat MK. Thermophilic fungi: their physiology and enzymes. Microbiology and Molecular Biology Reviews 2000; 64:461–488. https://doi.org/10.1128/MMBR.64.3.461-488.2000
35. Joan LC, James MC. Heterologous protein expression in the methylotrophic yeast *Pichia pastoris*. FEMS Microbiology Reviews. 2000; 24:45–66. https://doi.org/10.1016/S0168-6445(99)00029-7
36. Kristjansson MM, Kinsella JE. Protein and enzyme stability: structural, thermodynamic, and experimental aspects. Advances in Food and Nutrition Research. 1991; 35:237–316. https://doi.org/10.1016/S1043-4526(08)60066-2
37. Voutilainen SP, Nurmi-Rantala S, Penttila M, Koivula A. Engineering chimeric thermostable GH7 cellobiohydrolases in *Saccharomyces cerevisiae*. Applied Microbiology and Biotechnology. 2014; 98:2991–3001. https://doi.org/10.1007/s00253-013-5177-2
38. Marie C, Julia F, Mireille H, David N, Laurence L, Pedro MC, Jean-Guy B. A thermostable GH45 endoglucanase from yeast: impact of its atypical multimodularity on activity. Microbial Cell Factories. 2011; 10:103–114. https://doi.org/10.1186/1475-2859-10-103

39. Ishida T, Yaoi K, Hiyoshi A, Igarashi K, Samejima M. Substrate recognition by glycoside hydrolase family 74 xyloglucanase from the basidiomycete *Phanerochaete chrysosporium*. The FEBS Journal. 2007; 274:5727–5736. https://doi.org/10.1111/j.1742-4658.2007.06092.x

40. Berezina OV, Herlet J, Rykov SV, Kornberger P, Zavyalov A, Kozlov D, Sakhibgaraeva L, Krestyanova I, Schwarz WH, Zverlov VV, Liebl W, Yarotsky SV. Thermostable multifunctional GH74 xyloglucanase from *Myceliophthora thermophila*: high-level expression in *Pichia pastoris* and characterization of the recombinant protein. Applied Microbiology and Biotechnology. 2017; 101:5653–5666. https://doi.org/10.1007/s00253-017-8297-2

41. Damasio AR, Rubio MV, Goncalves TA, Persinoti GF, Segato F, Prade RA, Contesini FJ, de Souza AP, Buckeridge MS, Squina FM. Xyloglucan breakdown by endo-xyloglucanase family 74 from *Aspergillus fumigatus*. Applied Microbiology and Biotechnology. 2017; 101:2893–2903. https://doi.org/10.1007/s00253-016-8014-6

42. Matsuzawa T, Saito Y, Yaoi K. Key amino acid residues for the endo-processive activity of GH74 xyloglucanase. FEBS Letters. 2014; 588:1731–1738. https://doi.org/10.1016/j.febslet.2014.03.023

43. Arnal G, Stogios PJ, Asohan J, Skarina T, Savchenko A, Brumer H. Structural enzymology reveals the molecular basis of substrate regiospecificity and processivity of an exemplar bacterial glycoside hydrolase family 74 endo-xyloglucanase. The Biochemical Journal. 2018; 475:3963–3978. https://doi.org/10.1042/BCJ20180763

44. Lehtio J, Sugiyama J, Gustavsson M, Fransson L, Linder M, Teeri TT. The binding specificity and affinity determinants of family 1 and family 3 cellulose binding modules. Proceedings of the National Academy of Sciences. 2003; 100:484–489. https://doi.org/10.1073/pnas.212651999

45. Zhang Y, Yang F, Hu FH, Song JL, Wu SF, Jin YC. Binding preference of family 1 carbohydrate binding module on nanocrystalline cellulose and nanofibrillar cellulose films assessed by quartz crystal microbalance. Cellulose. 2018; 25:3327–3337. https://doi.org/10.1007/s10570-018-1803-6

46. Kraulis JP, Clore GM, Nilges M, Jones TA, Pettersson G, Knowles J, Gronenborn AM. Determination of the three-dimensional solution structure of the C-terminal domain of cellobiohydrolase 1 from *Trichoderma reesei*. A study using nuclear magnetic resonance and hybrid distance geometry-dynamical simulated annealing. Biochemistry. 1989; 28:7241–7257. https://doi.org/10.1021/bi00444a016

47. Dammak A, Quemener B, Bonnin E, Alvarado C, Bouchet B, Villares A, Moreau C, Cathala B. Exploring architecture of xyloglucan cellulose nanocrystal complexes through enzyme susceptibility at different adsorption regimes. Biomacromolecules. 2015; 16:589–596. https://doi.org/10.1021/bm5016317

48. Zheng F, Ding SJ. Processivity and enzymatic mode of a glycoside hydrolase family 5 endoglucanase from *Volvariella volvacea*. Applied and Environmental Microbiology. 2013; 79:989–996. https://doi.org/10.1128/AEM.02725-12

49. Kurasin M, Valjamae P. Processivity of cellobiohydrolases is limited by the substrate. The Journal of Biological Chemistry. 2011; 286:169–177. https://doi.org/10.1074/jbc.M110.161059

50. Nikolic M, Mojovic L. Characterization and degradation of pectin derived from Budimka apple. Journal of the Serbian Chemical Society. 2008; 73:157–167. https://doi.org/10.2298/JSC0802157N

51. Jiang KK, Li LL, Long LK, Ding SJ. Comprehensive evaluation of combining hydrothermal pretreatment (autohydrolysis) with enzymatic hydrolysis for efficient release of monosaccharides and ferulic acid from corn bran. Industrial Crops and Products. 2018; 113:348–357. https://doi.org/10.1016/j.indcrop.2018.01.047

52. Gao L, He X, Guo Y, Wu Z, Zhao J, Liu G, Qu Y. Combinatorial engineering of transcriptional activators in *Penicillium oxalicum* for improved production of corn-fiber-degrading enzymes. Journal of Agricultural and Food Chemistry. 2021; 69:2539–2548. https://doi.org/10.1021/acs.jafc.0c07659

53. Schmitz E, Leontakianakou S, Norlander S, Nordberg Karlsson E, Adlercreutz P. Lignocellulose degradation for the bioeconomy: The potential of enzyme synergies between xylanases, ferulic acid esterase and laccase for the production of arabinoxylo-oligosaccharides. Bioresource Technology. 2022; 343:126114. https://doi.org/10.1016/j.biortech.2021.126114
54. Valério R, Serra ATe, Baixinho J, Cardeira M, Fernández N, Bronze MR, Duarte LC, Tavares ML, Crespo JG, Brazinha C. Combined hydrothermal pre-treatment and enzymatic hydrolysis of corn fibre: Production of ferulic acid extracts and assessment of their antioxidant and antiproliferative properties. Industrial Crops and Products. 2021; 170:113731. https://doi.org/10.1016/j.indcrop.2021.113731
55. Appeldoorn MM, Kabel MA, Van Eylen D, Gruppen H, Schols HA. Characterization of oligomeric xylan structures from corn fiber resistant to pretreatment and simultaneous saccharification and fermentation. Journal of Agricultural and Food Chemistry. 2010; 58:11294–11301. https://doi.org/10.1021/jf102849x
56. Skinner RC, Gigliotti JC, Ku KM, Tou JC. A comprehensive analysis of the composition, health benefits, and safety of apple pomace. Nutrition Reviews. 2018; 76:893–909. https://doi.org/10.1093/nutrit/nuy033
57. Curci N, Strazzulli A, Iacono R, De Lise F, Maurelli L, Di Fenza M, Cobucci-Ponzano B, Moracci M. Xyloglucan oligosaccharides hydrolysis by exo-acting glycoside hydrolases from hyperthermophilic microorganism *Saccharolobus solfataricus*. International Journal of Molecular Sciences. 2021; 22:3325. https://doi.org/10.3390/ijms22073325
58. Zhang YHP, Cui JB, Lynd LR, Kuang LR. A transition from cellulose swelling to cellulose dissolution by o-phosphoric acid: evidence from enzymatic hydrolysis and supramolecular structure. Biomacromolecules. 2006; 7:644–648. https://doi.org/10.1021/bm050799c
59. Rose DJ, Inglett GE. Production of feruloylated arabinoxylo-oligosaccharides from maize (Zea mays) bran by microwave-assisted autohydrolysis. Food Chemistry. 2010; 119:1613–1618. https://doi.org/10.1016/j.foodchem.2009.09.053
60. Chapla D, Pandit P, Shah A. Production of xylooligosaccharides from corncob xylan by fungal xylanase and their utilization by probiotics. Bioresource Technology. 2012; 115:215–221. https://doi.org/10.1016/j.biortech.2011.10.083
61. Long LK, Xu MJ, Shi YX, Lin QY, Wang J, Ding SJ. Characterization of two new endo-beta-1,4-xylanases from *Eupenicillium parvum* 4–14 and their applications for production of feruloylated oligosaccharides. Applied Biochemistry and Biotechnology. 2018; 186:816–833. https://doi.org/10.1007/s12010-018-2775-6
62. Thomas MW, Mahalingeshwara BK. Methods for measuring cellulase activities. Methods in Enzymology. 1988; 160:87–112. https://doi.org/10.1016/0076-6879(88)60109-1
63. Furtado GP, Lourenzoni MR, Fuzo CA, Fonseca-Maldonado R, Guazzaroni ME, Ribeiro LF, Ward RJ. Engineering the affinity of a family 11 carbohydrate binding module to improve binding of branched over unbranched polysaccharides. International Journal of Biological Macromolecules. 2018; 120:2509–2516. https://doi.org/10.1016/j.ijbiomac.2018.09.022
64. Sluiter A, Hames B, Ruiz R, Scarlata C, Sluiter J, Templeton D, Crocker D. Determination of structural carbohydrates and lignin in biomass. Laboratory Analytical Procedure 2008.
65. Chen KX, Liu XC, Long LK, Ding SJ. Cellobiose dehydrogenase from *Volvariella volvacea* and its effect on the saccharification of cellulose. Process Biochemistry. 2017; 60:52–58. https://doi.org/10.1016/j.procbio.2017.05.023

Figures

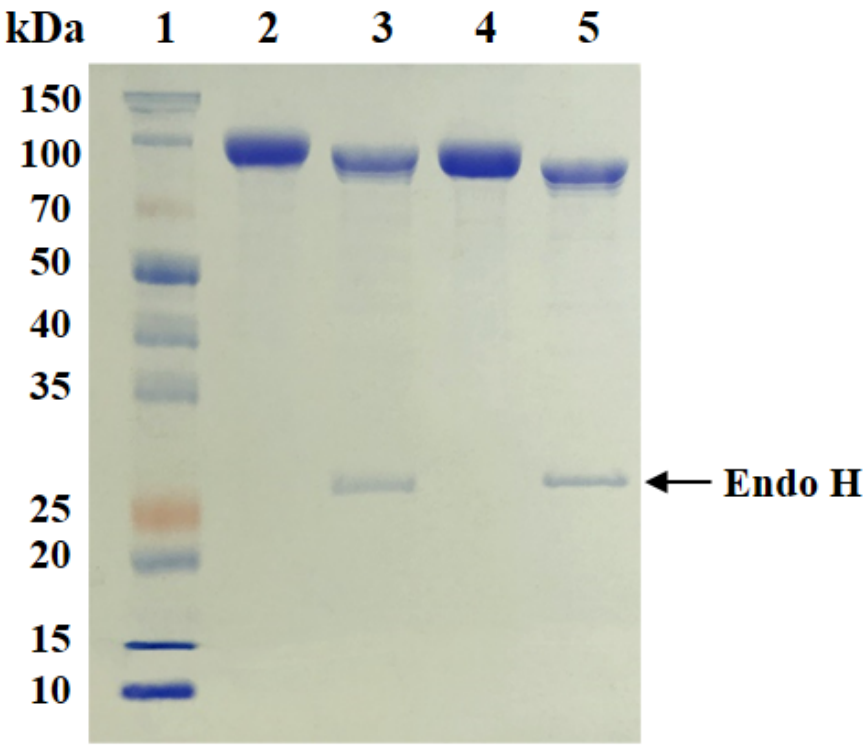

Figure 1

SDS-PAGE analysis of the purified *Tt*GH74 and *Tt*GH74ΔCBM, and endo H-treated *Tt*GH74 and *Tt*GH74ΔCBM. Lane 1, molecular mass marker; Lane 2, *Tt*GH74; Lane 3, endo H-treated *Tt*GH74; Lane 4, *Tt*GH74ΔCBM; Lane 5, endo H-treated *Tt*GH74ΔCBM.

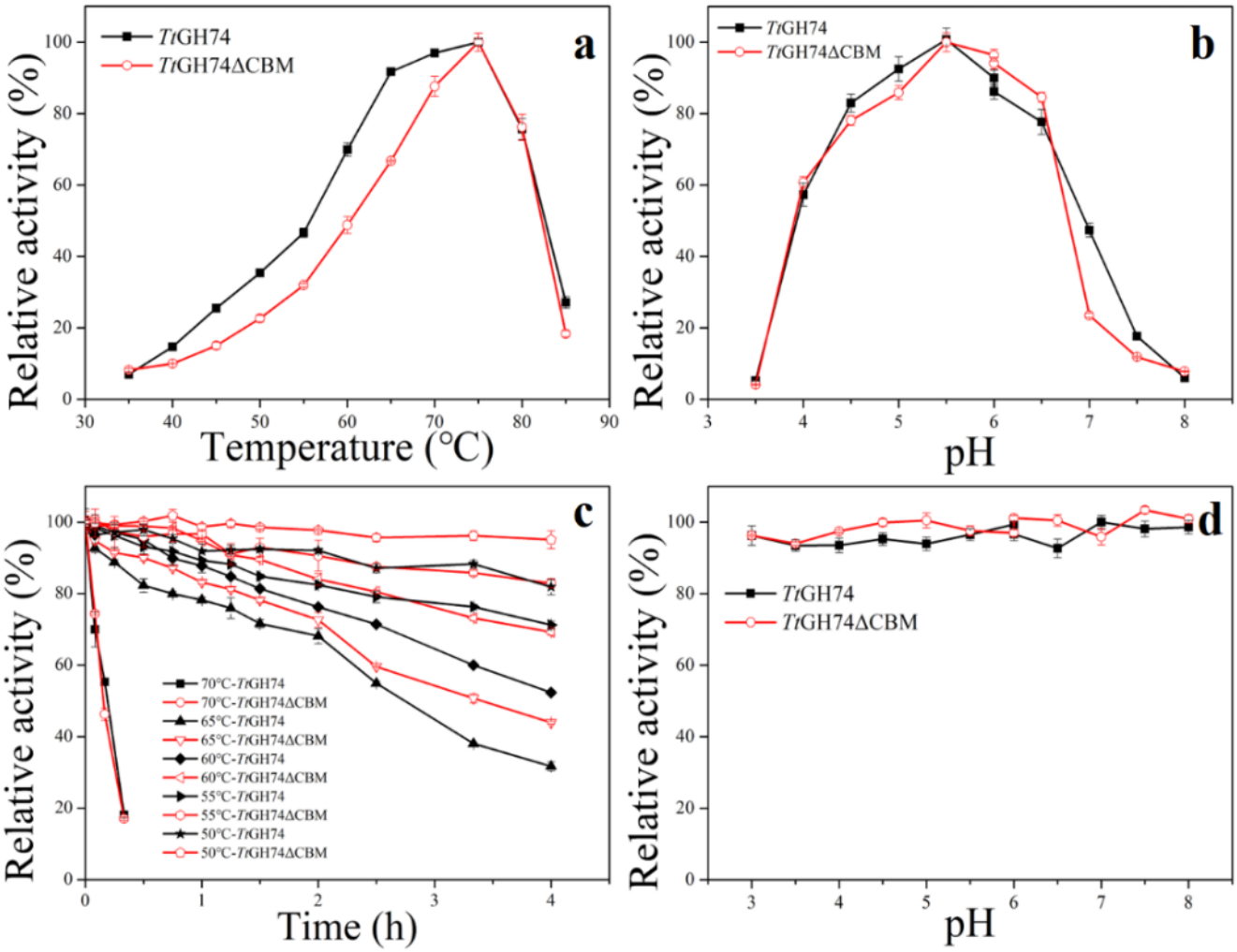

Figure 2

Effects of temperature (a) and pH (b) on enzyme activity, and effect of temperature (c) and pH (d) on stability of *Tt*GH74 and *Tt*GH74ΔCBM.

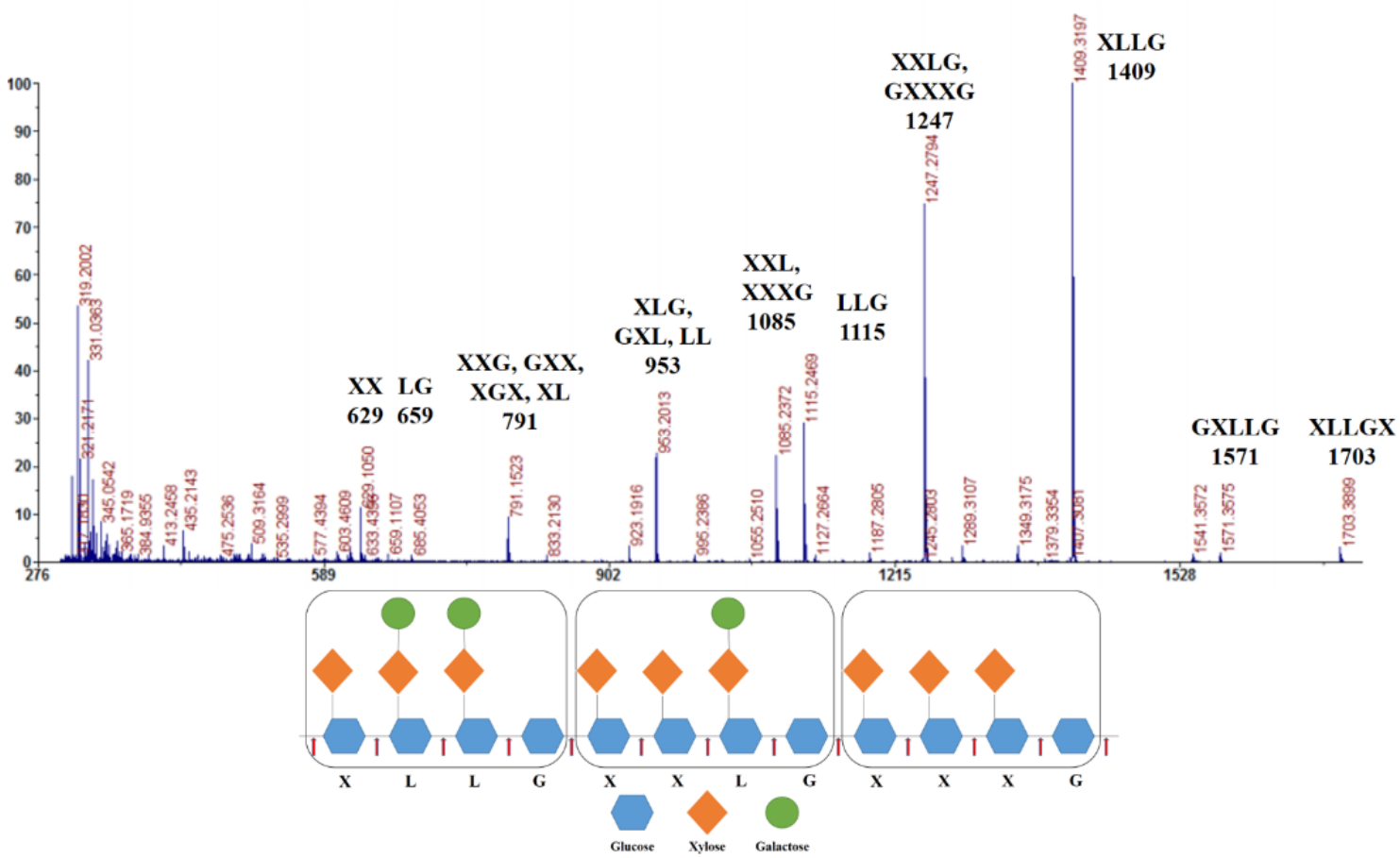

Figure 3

MALDI-TOF MS analysis of the products generated by *Tt*GH74 from tamarind seed XG. The bottom schematic diagram illustrates the possible XG cleavage patterns of *Tt*GH74.

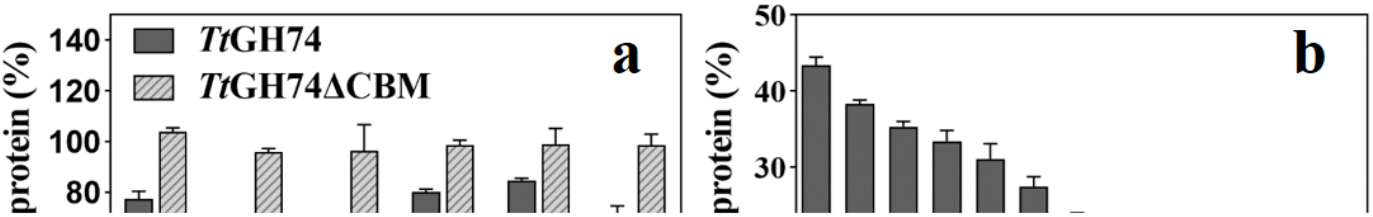

Figure 4

The adsorption differences of *Tt*GH74 and *Tt*GH74ΔCBM on various celluloses and lignocelluloses (a), the adsorption of *Tt*GH74 on cellulose with different proportions of XG (b), and analysis of their adsorption capacities on XG by electrophoresis in 7.5 % native polyacrylamide gel without xyloglucan (c) or with 0.005 w/v xyloglucan (d). Lane 1, *Tt*GH74; Lane 2, *Tt*GH74ΔCBM.

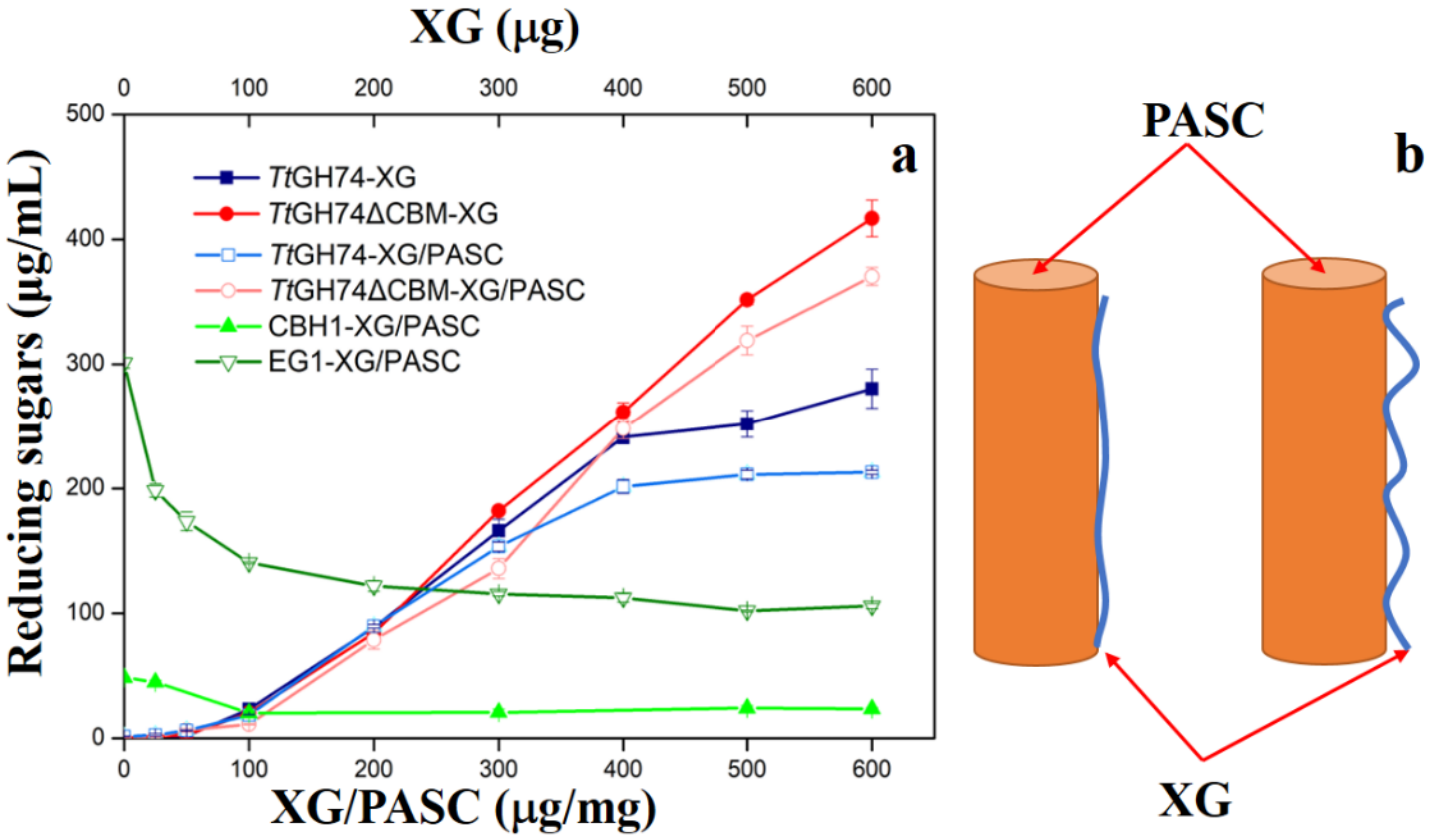

Figure 5

Hydrolysis of *Tt*GH74 and *Tt*GH74ΔCBM on different amounts of XG, and *Tt*GH74, *Tt*GH74ΔCBM, EG1, CBH1 hydrolyze PASC coated with different proportions of XG, respectively (a). The schematic diagram of the association pattern of XG and PASC (b). Orange cylinders represent PASC, XG is represented by a blue line. The left diagram shows the low proportion of XG/PASC, and the right diagram shows the high proportion of XG/PASC.

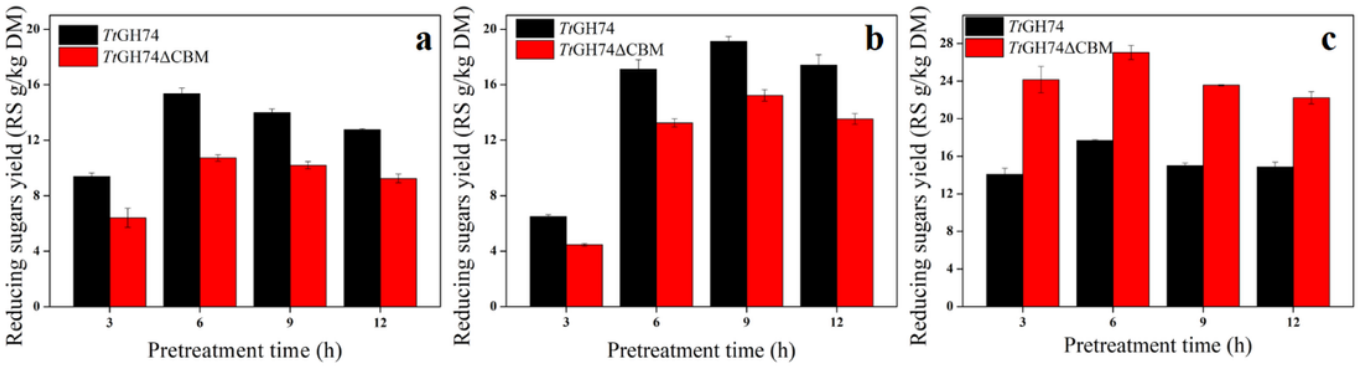

Figure 6

*Tt*GH74 and *Tt*GH74ΔCBM enzymatic hydrolysis of sulfuric acid pretreated-corn bran (a), DES pretreated-corn bran (b) and DES pretreated-apple pomace (c) with different pretreatment times.

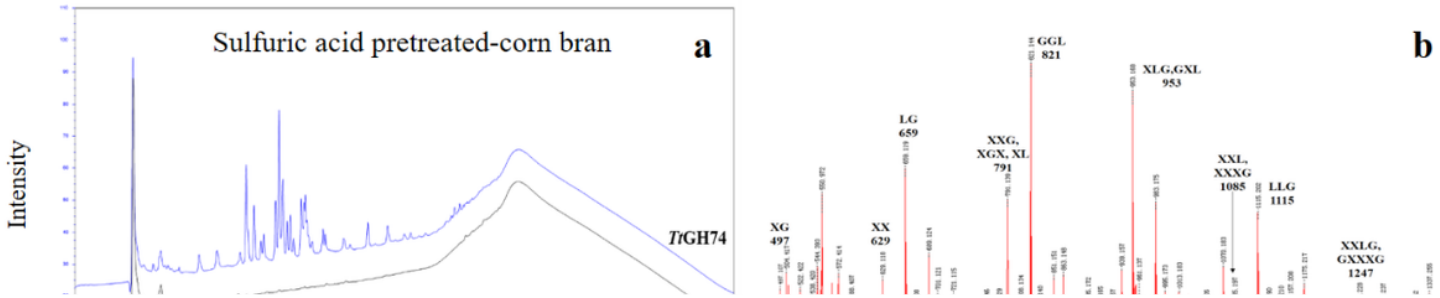

Figure 7

HPAEC-PAD (left) and MALDI-TOF MS (right) analysis of end-products generated by *Tt*GH74 from sulfuric acid pretreated-corn bran (a, b), DES pretreated-corn bran (c, d) and apple pomace (e, f).

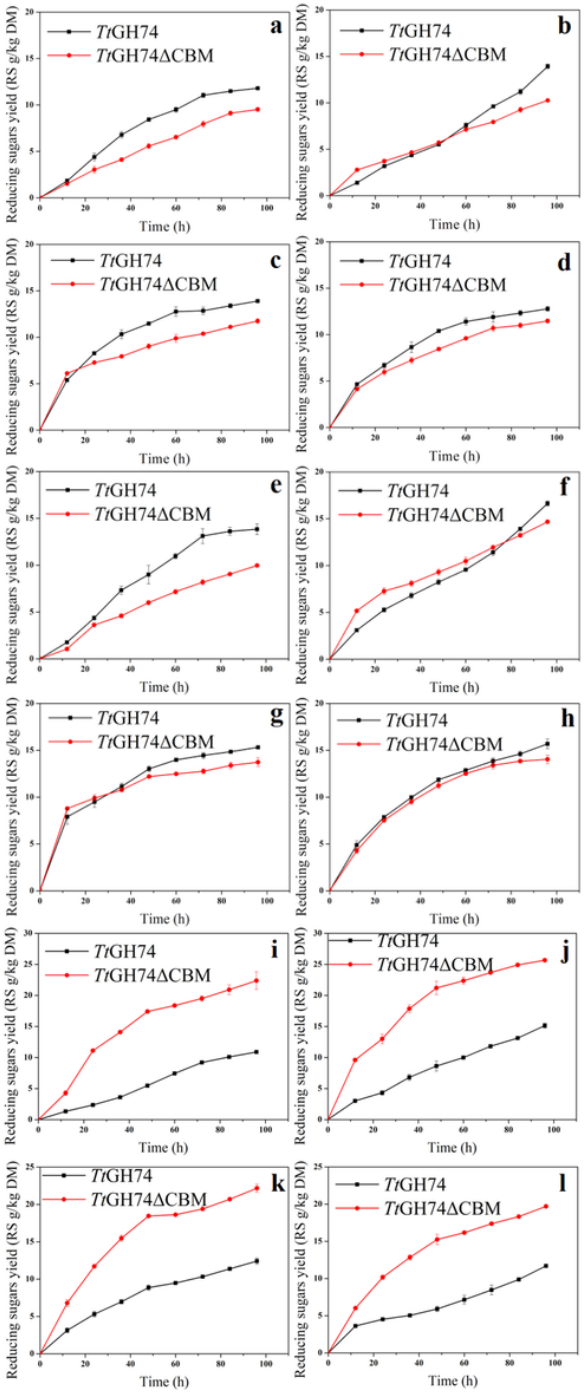

Figure 8

Time course of enzymatic hydrolysis of sulfuric acid pretreated-corn bran, DES-pretreated corn bran and apple pomace by *Tt*GH74 or *Tt*GH74ΔCBM. a-d: 10, 20, 40, and 80 mg of sulfuric acid pretreated-corn bran, respectively; e-h: 10, 20, 40, and 80 mg of DES pretreated-corn bran, respectively; i-l: 10, 20, 40, and 80 mg of DES pretreated-apple pomace, respectively.

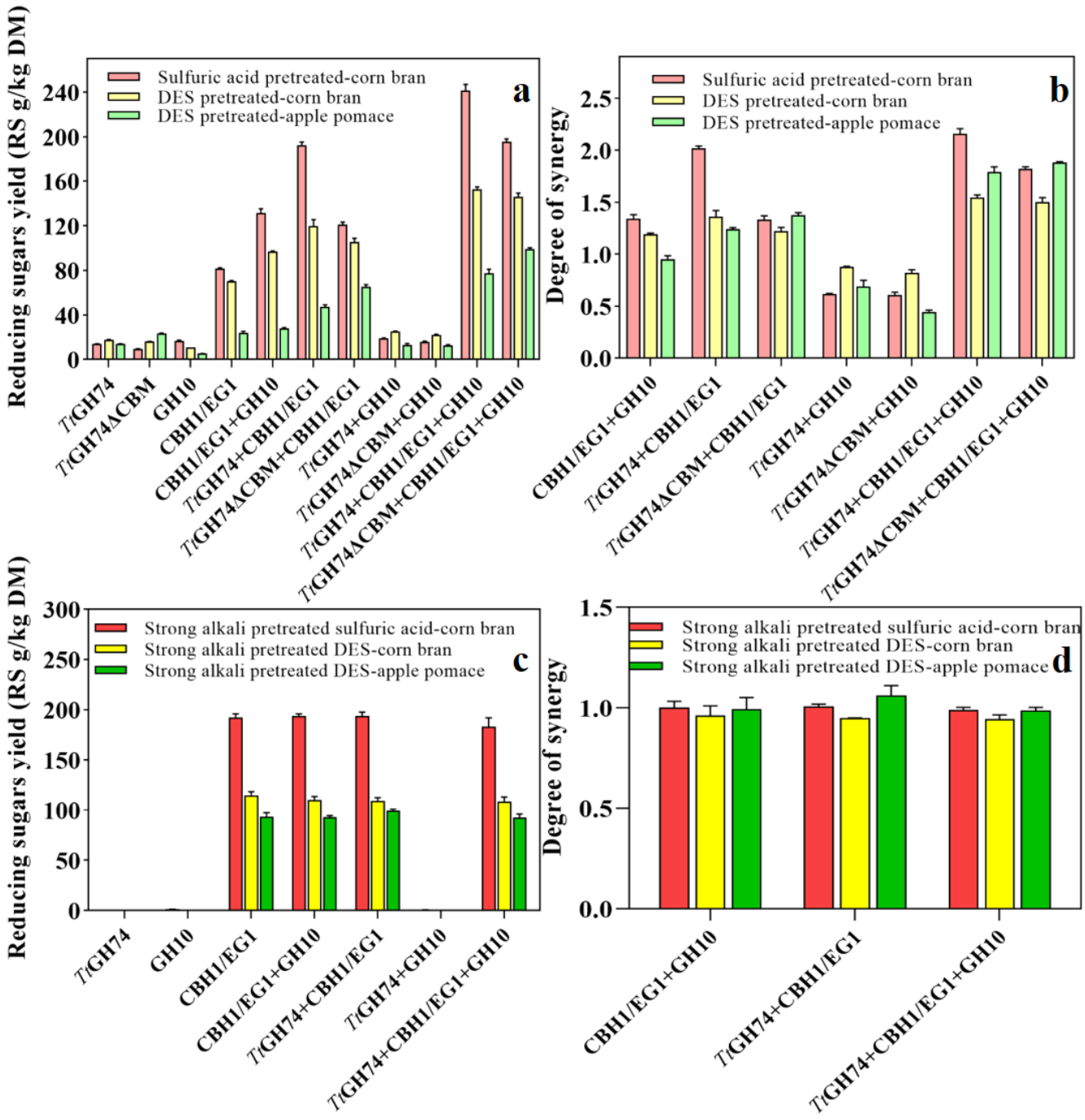

Figure 9

The synergy between *Tt*GH74, *Tt*GH74ΔCBM and GH10 xylanase, CBH1/EG1 mixture on sulfuric acid pretreated-corn bran and DES pretreated-lignocellulose (a, b). Enzymatic hydrolysis verification of pretreated-lignocellulose components treated by strong alkali (c, d).

Supplementary Files

This is a list of supplementary files associated with this preprint. Click to download.

- Additionalfile1final.docx
- Additionalfile2.docx
- Additionalfile3.docx
- Additionalfile4.docx
- Additionalfile5.docx
- Additionalfile6.docx